

**Listen! It's a phase transition.**  
**The sound of a shape-memory alloy.**

Carlo Andrea Rozzi

*CNR — Istituto Nanoscienze, via Campi 213/a, 41125 Modena, Italy\**

Annamaria Lisotti

*Dipartimento di Scienze Fisiche, Informatiche e Matematiche,  
Università di Modena e Reggio Emilia,  
via Campi 213/a, 41125 Modena, Italy*

Guido Goldoni and Valentina De Renzi

*Dipartimento di Scienze Fisiche, Informatiche e Matematiche,  
Università di Modena e Reggio Emilia,  
via Campi 213/a, 41125 Modena, Italy and*

*CNR — Istituto Nanoscienze, via Campi 213/a, 41125 Modena, Italy\**

**Abstract**

The remarkable properties and numerous technological applications of shape-memory alloys are due to a solid-to-solid phase transition involving a temperature-driven rearrangement of their crystal structure. Here, we propose a simple, yet effective experiment probing the *sound* emitted by a  $\text{Ni}_{40}\text{Ti}_{50}\text{Cu}_{10}$  bar at different temperatures crossing the transition between martensite and austenite phases and we discuss the relationship with the elastic properties of the material. We show that the phase transition, which occurs slightly above room temperature, can be qualitatively monitored by the ear and that a quantitative description of the phenomenon can be obtained using a very simple setup and sound analysis tools. We argue that such a sound-based investigation provides an unusual, stimulating way to experimentally introduce solid-to-solid phase transitions suitable for undergraduate courses.

## I. INTRODUCTION

Phase transitions (PTs) are ubiquitous phenomena.<sup>1</sup> In essence, a PT is the collective response of a statistical system<sup>2</sup> – a collection of a very large number of *interacting* elementary parts, such as atoms or molecules – to a small change of some external parameters, say, temperature, pressure, magnetic field, strain, etc. The familiar solid/liquid and liquid/gas transformations are just everyday examples and very effective ways to conceptualize PTs, which are signalled by a visible change in the particle density. Although not often emphasized in undergraduate studies, PTs are present in many material systems, simple examples being the nematic transition in liquid crystals, the order/disorder transition in binary alloys, the ferromagnetic transition in magnetic materials.<sup>2</sup> PTs also manifest themselves as quantum phenomena, such as the superconductivity shown by many metals or doped oxides at sufficiently low temperature and high pressure.<sup>3</sup>

In undergraduate physics and chemistry courses, the prototypical and most widely addressed case of PT is that of water transformations. Their importance cannot be overestimated; besides being a common experience, they play a crucial role in many fundamental phenomena in earth and life sciences, and technology. On the other hand, providing further examples of PTs - suitable to be investigated experimentally in a didactic lab - is instrumental to illustrate the generality and ubiquity of this class of phenomena.

The martensitic PT could represent such an example, with high pedagogical value;<sup>4</sup> it is a first order solid-to-solid PT<sup>5</sup> occurring, for example, in the Nickel-Titanium alloy (Nitinol) and its derivatives, belonging to the class of so-called Shape Memory Alloys (SMAs).<sup>6-8</sup> As shown in Fig. 1, it consists in a change of the microscopic crystalline structure, from cubic (austenite) to monoclinic (martensite), driven by temperature. The experimental study of the martensitic PT has several practical and didactic advantages. Nitinol is a solid, safe, easy to manage, cheap metal, available off-the-shelves. The transition occurs at a lab-suitable range of temperature (around  $\sim 50$  °C). Most interestingly, it underlies the astonishing shape-memory effect (SME),<sup>9</sup> a quite popular subject for classroom and science exhibits,<sup>10-12</sup> with numerous technological applications<sup>13-16</sup> which may easily trigger students' curiosity.

Besides the SME, the martensitic PT cannot be perceived by the eye, but has an important - though less explored - impact on the elastic and acoustic properties of the material,

which also has interesting technological applications in itself.<sup>17,18</sup> This can be immediately realized by dropping on the floor a small Nitinol bar, first in its austenite phase - i.e at temperatures above the transition - and then in its martensite phase (below the transition). As can be easily perceived by listening to the sound recordings *S2\_Temperature\_sounds.mp4*, provided as Supplementary Material, the former rings like a metallic object, characterized by a distinct pitch, while the latter produces a “thud” with a muffled sound and no definite pitch, resembling more the impact noise of a softer, non-metallic object.<sup>19</sup>

While it is a common experience for musicians to find their instrument slightly out of tune when they undergo environmental changes, in our case a moderate temperature change induces a very large frequency shift and turns an unpitched percussion (in the martensite phase) into a pitched one (in the austenite phase). Indeed, the nature of these two phenomena is completely different. While the former is explained in terms of simple thermal expansion effect, or by the temperature dependence of the speed of sound in air, the latter - as we will show in the following - can be quantitatively related to the martensitic PT. This simple yet astonishing finding naturally leads to inquire whether sonic data could be used as an alternative way to investigate the martensitic PT. Indeed, a few authors pursue this idea in a didactic context, but only in a qualitative way.<sup>20,21</sup>

In this paper, we show that the sound produced by a Nitinol sample can be continuously monitored throughout the PT using an elementary experimental setup, allowing to quantitatively correlate the pitch and timbre of the perceived sound with the phase state. Our approach shows that the PT is directly reflected in the properties of the emitted sound, though no visible macroscopic change in the material occurs. This conveys the idea that the material macroscopic properties arise at the nano-scale. Moreover, it provides an easy ‘real-time’ way to measure its elastic properties, which are usually only described in static terms and in an engineering context. It also allows students to access multiple indicators of the changes occurring within the material, both energy conserving (elasticity) and energy dissipating (damping). Lastly, and importantly from the didactic point of view, extending the realms of probes to sound waves offers the possibility of an interdisciplinary path joining the study of the material physical properties, such as elastic properties, to the physics of sound and to engineering applications, like damping, vibration and noise control in dynamical structures.

## II. THEORETICAL BACKGROUND

### A. Temperature dependence of the fundamental frequency in a thin bar of a common metal

This section briefly discusses how temperature affects the fundamental frequency of a bar in the case of ordinary metals, i.e. in a temperature range not affected by any phase transition. The fundamental frequency of a thin bar depends on its dimensions (length  $L$  and thickness  $h$  in the direction of the strike) and on the Young's modulus  $E$  of the material (see details in the Appendix) according to

$$\nu_0(T) \propto h^2(T) \sqrt{\frac{E(T)}{L^3(T)}}. \quad (1)$$

In the case of usual materials – as for instance Iron around room temperature - the temperature-induced change in the sound is therefore related to thermally-induced variations of the sizes of the bar, and of its Young's modulus according to

$$\frac{d\nu}{\nu} = 2 \frac{dh}{h} - \frac{3}{2} \frac{dL}{L} + \frac{1}{2} \frac{dE}{E}. \quad (2)$$

If we assume all these changes to be linear with temperature, the overall relative variation in the bar tuning reads as

$$\frac{d\nu}{\nu} = \frac{\alpha + \beta}{2} dT, \quad (3)$$

where  $\alpha = \frac{1}{dT} \frac{dL}{L} = \frac{1}{dT} \frac{dh}{h}$  is the coefficient of the linear thermal expansion and  $\beta = \frac{1}{dT} \frac{dE}{E}$  accounts for the Young's modulus first-order variation with temperature. For ordinary metals the values of  $\alpha$  and  $\beta$  are as small as  $10^{-5} \text{ }^\circ\text{C}^{-1}$  and  $10^{-4} \text{ }^\circ\text{C}^{-1}$ , respectively<sup>22,23</sup> (being  $\alpha$  positive and  $\beta$  negative). As we will show in Sec. IV A, this produces a tiny, essentially inaudible change in the fundamental frequency, for a temperature variation of few tens of Celsius degrees.

### B. The martensitic phase transformation in Nitinol

Solid-to-solid PTs connect two states of matter which differ in their crystallographic structure. Though these transformations consist in tiny atomic displacements – if compared to the interatomic distances – these subtle movements are responsible for dramatic changes

in the macroscopic properties of the material. The martensitic PT belongs to a paradigmatic class of diffusiveless transformations occurring in many materials, and in particular in metallic alloys. It is also called a “military” transformation because it occurs as an ordered, cooperative shear-like movement of atomic layers, rigidly shifting (sliding) with respect to neighboring planes.

Although in this paper we deal with the ternary alloy  $\text{Ni}_{40}\text{Ti}_{50}\text{Cu}_{10}$  (NiTiCu in the following), to visualize the microscopic nature of the martensitic PT, in Fig. 1 we show the simplest case of a SMA made of a binary alloy, with the two atomic species which alternate to compose likewise compenetrating lattices. At high temperature, the stable crystal structure is a cubic austenite [Fig. 1b)]. At low temperature the stable phase is a less symmetric monoclinic martensite [Fig. 1a)]<sup>24</sup>. Moreover, in the low-temperature phase each plane may slide, by the same monoclinic angle, either to the right or to the left, the two configurations having the same energy. Therefore, upon cooling from the austenite phase, the martensite phase may host twinned domains which break the translational invariance of the lattice and may scatter and attenuate sound waves. Moreover, in this state, if stress is isothermally applied, the twin layers switch easily (at almost no energy cost) to accommodate the applied stress by flipping twinned domains, and the sample can be plastically deformed to any shape. This characteristic of the martensitic phase plays a crucial role in the shape-memory effect<sup>25,26</sup>, which occurs in some inter-metallic compounds like Nitinol<sup>27</sup>, across the martensitic transformation. As the physics behind this particular fascinating effect is not the direct object of our investigation, it will not be further deepened here. The interested reader could refer to<sup>25,26</sup> for a thorough discussion. Simulations of the microscopic mechanisms underlying the austenite/martensite transformation for the NiTi binary material can be found in Ref. 28.

It is important for the following to highlight that - at variance with the better known water transformations - the temperature-induced austenite/martensite transformation is not isothermal;<sup>29,30</sup> upon cooling the austenite starts transforming into martensite at a “martensite start” temperature  $M_S$  and the process is completed at a “martensite finish” lower temperature  $M_F$ . This can be explained taking into account the influence of internal stress on the transition temperature, in analogy with the role of pressure on the liquid-vapour transition temperature of water.<sup>4</sup> Moreover, the presence of hysteresis - fingerprinting a first-order phase transition - can also be observed, i.e. upon heating, austenite starts forming at a

”austenite start” temperature  $A_S$ , different from  $M_F$ , and the process is completed at a ”austenite finish” temperature  $A_F$ , different from  $M_S$ . These temperatures are somewhat sample dependent, but normally fall in the range of a few tens of Celsius degrees for NiTi compounds.<sup>20</sup>

### III. MATERIALS AND METHODS

We employed custom made bars (though similar Nitinol sample bars are commercially available) with nominal stoichiometry  $\text{Ni}_{40}\text{Ti}_{50}\text{Cu}_{10}$ . Our bar was  $(20.0 \pm 0.1)$  cm long with an approximate rectangular cross section with sides  $(0.70 \pm 0.05)$  cm  $\times$   $(0.60 \pm 0.05)$  cm and a mass  $(51 \pm 1)$  g. At room temperature the sample was stable in its martensite phase. An additional cylindrical Iron bar,  $(20.2 \pm 0.1)$  cm long and with a diameter of  $(0.79 \pm 0.02)$  cm and mass  $(77 \pm 1)$  g, was used as a control sample.

The experimental procedure is sketched in Fig. 2. The bars were mounted on a suspension set allowing them to vibrate freely and, at the same time to be handled safely in and out hot water. Two cotton threads were used to hold the bars in position hanging at the nodes of the first free mode of vibration (see App. A). The bars were put in water at 70 °C, quickly extracted and let thermalize down to room temperature. Meanwhile, they were quickly repeatedly hit with a rubber hammer in the middle, perpendicularly to their length, to excite flexural vibrations. A thermocouple was attached to each bar near one node to monitor its temperature.

The impact sound was recorded with a USB microphone directly connected to a computer sound card. The sound spectrum and the frequency of the fundamental were measured using the open-source software Audacity<sup>31</sup>. The decay time of the hits was estimated performing a linear fit of the log plot of the sound pressure trace (see App. B for details). Alternative experimental setups are discussed in Sec. IV D.

## IV. RESULTS AND DISCUSSION

### A. Fundamental frequency of NiTiCu and Iron

As described in details in Sec. III, the change in the acoustic properties of a NiTiCu bar has been recorded upon decreasing its temperature across the NiTiCu martensitic PT

(between 65 °C and 24 °C), and compared with those of the control Iron bar. As immediately realized by the ear (listen to *S2\_Temperature\_sounds.mp4*, in the Supporting Information), while the Iron bar sound remains about the same (we employed a cylindrical bar with fundamental ring tone at about 876 Hz) as expected, the fundamental frequency of the NiTiCu bar decreases significantly while its temperature decreases. In Fig. 3 the recorded NiTiCu spectra are reported for selected temperature values, along with their corresponding scale, in musical notation, showing how the fundamental frequency decreases by almost 40% from roughly a sharp C<sub>5</sub> at 51 °C to a sharp E<sub>4</sub> at 30 °C. On the other hand, for temperatures outside this interval the intonation remains quite stationary. Moreover, for NiTiCu other important changes occur as the temperature decreases, namely: (i) the ringing time shortens, and (ii) the pitch sensation becomes more and more indefinite.

## B. Temperature dependence of elastic properties

The measured fundamentals of the Iron and NiTiCu bars are reported and compared in Fig. 4 at different temperatures. All data are obtained in a *cooling* sequence. For the 876 Hz ring tone of the Iron bar in Fig. 4, we observe an increase as small as 5 Hz as the temperature decreases by 40 °C. This variation goes unnoticed by the ear, since the detuning is very close to the just noticeable difference in pitch for a pure tone at the same frequency.<sup>32</sup> The slight decrease with temperature, with a slope of -0.1 Hz °C<sup>-1</sup>, is well described by Eq. 3, with tabulated values of  $\alpha$  and  $\beta$ .<sup>23</sup>

The case of NiTiCu is qualitatively very different: the NiTiCu fundamental drops abruptly upon cooling between  $M_S = 43$  °C and  $M_F = 32$  °C. This change fingerprints the occurrence of the martensitic PT. The corresponding average slope is 23 Hz °C<sup>-1</sup>, more than two orders of magnitude larger than the Iron one, and with opposite sign.

The observed sudden decrease in frequency upon cooling can be in principle attributed to an abrupt change in either the dimensions of the bar (and correspondingly, its density), or the Young's modulus, or both. However, since the densities of martensite and austenite NiTiCu alloys differ by less than 5%,<sup>33</sup> we can safely conclude that density increase has a minor effect, and that the pitch drop should be essentially attributed to a strong variation in the Young's modulus across the PT – that is to say, austenite is much stiffer than martensite.

By using Eqs. (A1) and (A2) in App. A, we can estimate the value of the Young's

modulus, as shown in Fig.5. From the lowest and highest frequencies (respectively found at temperature lower than  $M_F$  and higher than  $M_S$ ) we obtain  $E_m = (26 \pm 1)$  GPa and  $E_a = (69 \pm 1)$  GPa, in fair agreement with literature, which reports values  $< 40$  GPa for martensite and  $60 - 90$  GPa for austenite in Nitinol.<sup>34-36</sup> The observed temperature dependence of the Young's modulus can be rationalized recalling that the martensite and austenite phases coexist throughout the transition, so that – at each temperature  $M_S > T > M_F$  – the effective Young's modulus can be expressed as a linear combination of the martensite ( $E_m$ ) and austenite ( $E_a$ ) values. Introducing  $\xi(T)$  as the fractional amount of martensite at temperature  $T$ , the effective Young's modulus reads as

$$E_{\text{eff}}(T) = \xi(T)E_m + [1 - \xi(T)]E_a = E_a - [E_a - E_m]\xi(T), \quad (4)$$

where  $\xi(T)$  can be expressed as the logistic curve

$$\xi(T) = \frac{1}{1 + e^{-k(T-T_m)}} \quad (5)$$

with  $T_m$  and  $k$  representing the temperature midpoint and the logistic growth rate, respectively. Indeed, as shown in Fig.5, the experimental data can be nicely interpolated using Eqs. (4) and (5), with  $T_m$  and  $k$  as fitting parameters (see caption for details).

At a microscopic level, the frequency shift can be understood in terms of the rearrangement in the unit cell occurring at the PT. Different atomic coordination corresponds to substantially different effective elastic potential between atoms, i.e. different amount of elastic energy per volume in the material.

### C. The transition from unpitched to pitched sound

So far we have focused on the fundamental frequency of the bar, highlighting its relationship with the phase of the material. When the NiTiCu bar is cooled, the fundamental frequency decreases, and, correspondingly, the pitch becomes lower. However, at some point, the sensation disappears and the sample does not seem to have a definite pitch any longer. This change is perceived despite the fact that a peak for the fundamental is still clearly distinguishable in the spectrum of the emitted sound, and a regular oscillation can be easily recognized by looking at the recorded waveform [see Fig. 3 and 6 ( middle and top panels)]. Such a change is not due to a strong change in the structure of the overtones, which maintain



the same ratios with the fundamental at all temperatures (see App. A).

Therefore, the timbral change from a “ring” sound into a “thud” must be correlated with the sound duration; that is, a definite pitch is perceived only if the bar is vibrating long enough. This feature is shown in Fig. 6 (bottom panel), which depicts the envelopes of two recorded waveforms corresponding to austenite and martensite. The logarithmic scale in the vertical axis (proportional to the sound pressure level) shows that the sounds decay at an exponential rate, with very different time constants for the two phases; the austenite decay time is about one order of magnitude longer than the martensite one (about 100 ms vs 10 ms).

The different decay time of the two phases is related to a drastic change in the damping coefficient of the elastic oscillations of the bar. Generally speaking, the damping coefficient is due to dissipation of mechanical energy and may have different sources, collected under the name of “friction”. Here only internal friction, namely, the dissipation of elastic energy caused by the internal forces, is at play. External sources of friction, such as the viscous drag by air or friction at the support points, are not supposed to change between the martensite and austenite phase, as the transition does not affect the macroscopic shape of the bar.<sup>37</sup>

Internal damping indicates how fast elastic energy is dissipated into heat in the material. In a cycle of vibrations the bar undergoes a periodic sequence of stress and strain. A little internal hysteresis loss occurs within each full oscillation, and some elastic energy is lost to heat. Internal friction in metals and alloys is particularly sensitive to defects in the lattice and to their mobility. This picture naturally fits the scenario of a progressively vanishing sensation of pitch when proceeding from austenite to martensite. In fact, in the martensite phase domains and twin boundaries form an irregular pattern, which can move easily and are good sources of energy dissipation, while the ordered lattice of the more rigid austenite phase responds elastically to external perturbations. More details on the subject of damping in shape memory alloys and their application can be found, for example, in Refs. 38–40 and references therein.

In order to follow the change in the dissipated energy as a function of temperature, we have evaluated the  $Q$  factor of the fundamental resonance (see the definition in App. B). Fig. 7 shows  $Q^{-1}$  (which is a direct indicator of dissipation) as a function of temperature for the NiTiCu and Fe rods. While the value for the Iron sample is almost constant, the NiTiCu sample roughly doubles its dissipation throughout the temperature span considered.

Although the uncertainty in the estimation of  $Q$  is higher than the one for the frequency, especially at low temperatures, our data clearly show the trend of increasing  $Q^{-1}$  for decreasing temperature, which corresponds to the decrease in the decay time when the temperature is lowered.

These data demonstrate that the utterly different damping properties of martensite and austenite phases can be emphasized by studying the sound decay time of the sound recordings. The steps for a quantitative estimation of  $Q$  are explained in App. B. However, the Audacity software allows the user to simply visualize the wave form in a dB scale, as shown in Fig. 6 and can be a useful tool in a didactic context.

#### **D. Remarks about the experimental setup**

Suspending the bars with thin strings by the nodes allows to best approximate the free-boundary conditions, and to achieve the longest ringing times. We have also explored different setups and procedures, each having pros and cons.

For instance, one could choose to firmly clamp the bar at one nodal point. This provides rather repeatable sounds, at the price of a stronger damping, i.e. a smaller signal to noise ratio in an ordinarily quiet room [about 40 dB(A)]. Moreover, the microphone placement is more critical here than in the former case. Anyhow, one should bare in mind that the thin bars are not optimized for sound radiation, as it happens for actual musical instruments. For this reason, while the sensation of sound and pitch is quite striking when listening to the recording, in the room it rapidly fades away even at moderate distances from the vibrating bar.

Alternatively, to achieve quicker handling, the bars could be gently held at a nodal point by the experimenter's fingers (suitably gloved for heat insulation) and even hit at one side with the bare knuckles of the other hand.<sup>41</sup> This handling has the didactic advantage of adding a touch feeling to the experience of vibration. It also makes possible to keep the bar close to the experimenter's ear, where its sound is better perceived, and it minimizes waiting time with respect to a fixed-clamping device. However the amount of friction at the holding point cannot be precisely controlled, and will affect the accuracy in the measurement of damping (see the discussion in Sec. IV C). In all cases, it is suggested to find and mark in bright color the nodal points (see App. A) and the middle point of the bar.

In order to simplify the sound signal processing and analysis we recommend to use bars with rectangular, instead of squared cross section. The larger aspect ratio helps keeping the frequencies of the bending vibrations in the two orthogonal dimensions perpendicular to the bar length more far apart and prevents the appearance of beats during the decay phase, which may obscure the exponential decay envelope of each mode. It also makes the sound radiation from one side slightly weaker than the other.

Moreover it is desirable to have someone with a musically trained ear assisting, to help assessing the quality of the sound while recording, and spotting interference from the environment in the frequency band 300-800 Hz. Finally, be aware that the decay time constant hugely varies both with materials and across temperatures. For NiTiCu, it spans an interval from about 300 ms down to 13 ms, while for Iron it is stable at about 600 ms. When recording multiple strikes, be sure to allow the sound to be completely damped before proceeding to the next strike, while monitoring the temperature.

## V. CONCLUSIONS

In summary, we have shown that an accurate description of the macroscopic effects of the martensitic phase transition can be achieved through a quite straightforward investigation of the acoustic properties of a NiTiCu thin bar, as compared with those of a normal metal, i.e. Iron. With a minimal setup, students experience that the elasticity of a NiTiCu bar depends critically on its phase. When the transition temperature is crossed, the frequency markedly changes, corresponding to a steep variation in the Young's modulus of the material. The striking difference between NiTiCu and Iron elastic and acoustic behavior as a function of temperature allows students to realize how the former can only be explained by a phase change.

Therefore, this experiment provides a novel way to explore the characteristic features of a first-order (solid-solid) phase transition. Although the detailed microscopic analysis of this phenomenon is out of the scope of the present work, the possibility of capturing a change in the unit cell symmetry just by listening to the sound made when a bar is hit is a great stimulus to discussion about the intimate linking between the properties of matter at the atomic level and their macroscopic behavior. This experience builds on, and extends to a new sensorial domain the phenomenology of PTs. In combination to a rather simple equipment

giving students full operative control, this makes the present experimental approach suited to a Modern Physics Laboratory course both in a physics major and in interdisciplinary curricula.

We finally note that martensitic PTs are usually presented and discussed in the context of the SME. This is indeed a fascinating subject for students, but its complex relationship to the PT is somewhat cumbersome and not so easy to explain. To this respect, the present approach, which does not rely on an explicit discussion of SME, has the advantage of a more straightforward link between the measured properties of the emitted sound, with no visible macroscopic change in the material, and the fundamental features of the PT itself.

### **Appendix A: Acoustics of thin bars**

Metal or wooden thin beams or bars of several shapes are used in both percussion instruments such as Marimba, Xylophone, Glockenspiel, etc., and (as flat lamellae) in reed wind instruments such as Reed Organ, Harmonica, Accordion, etc. In percussions the bars are set to vibration by striking them with a hammer, while in winds by the action of an air flow. In both cases the excitation slightly deforms the bar. Due to the elasticity of the material, the mechanical energy stored into the initially deformed shape is partially transformed into elastic waves propagating along the bar, and part of the wave energy is eventually radiated into the air as sound.

As a first approximation the bending normal modes of a free thin bar are calculated in the Euler-Bernoulli beam approximation, (i.e. considering the bending moment as the only source of restoring elastic force). The frequencies of the normal modes can be expressed as the product of three factors accounting respectively for the shape, size and material of the bar. The fundamental frequency of the bending vibration of a free bar having constant cross-section is

$$\nu_0 = A \frac{h}{L^2} c, \tag{A1}$$

where  $L$  is the length of the bar,  $h$  its thickness in the direction of the strike, and  $A$  is a constant accounting for the shape of the cross-section.<sup>42</sup> For a bar with rectangular cross section  $A = 1.028$ . For the circular cross section  $A = 0.890$ .  $c$  is the speed of a longitudinal elastic wave traveling in the bulk material, “speed of sound” in brief, which only depends

on two properties of the material itself, namely, its density  $\rho$  and its Young's modulus  $E$  as

$$c = \sqrt{\frac{E}{\rho}}. \quad (\text{A2})$$

The higher frequency modes are in non-harmonic ratios to the fundamental frequency. The constants for each overtone are different, but depend only on the boundary conditions and shape, and not on the material properties, therefore the overtone frequency distribution does not depend on temperature.

This simple model is sufficiently accurate in the thin beam limit, i.e. when  $\lambda \gg 2\pi K$ , where  $K$  is the gyration radius of the beam, and  $\lambda$  the wavelength of the mode, which is the case for our test bar, since, at least for the fundamental mode it yields

$$\frac{2\pi K}{\lambda} \approx \frac{\pi h}{\sqrt{12L}} = 0.003. \quad (\text{A3})$$

As a reference, the expected fundamental of our Iron bar can be found by substituting in (A2) tabulated standard data for Iron ( $\rho = 7800 \text{ kg m}^{-3}$  and  $E = 211 \text{ GPa}$ ) and the circular section shape factor for  $A$ . Equation (A1) then returns a frequency of 895 Hz, within about 2% from to the measured one of 876 Hz. The Iron sample at room temperature produces a clearly ringing  $A_5$  note (which is nominally at 880 Hz).

We can make the temperature dependence of  $\nu_0$  explicit by substituting in (A2) the density

$$\rho = \frac{m}{h^2 L}, \quad (\text{A4})$$

where  $m$  is the mass of the bar. Therefore, assuming the shape remains unchanged, the fundamental frequency can be expressed as a function of temperature-dependent variables as

$$\nu(T) \propto h^2(T) \sqrt{\frac{E(T)}{L^3(T)}}. \quad (\text{A5})$$

The position of the nodal points of each mode of vibration can also be analytically determined for the ideal thin bar model, and, for the fundamental mode, the nodes are located at a distance of  $0.224 \cdot L$  from each end of the bar<sup>42</sup>. This fact can be profitably exploited in the experiments to enhance the pitch sensation. In fact the sound spectrum of the struck bar is composed of a wide-band impact noise, and of a sequence of distinct overtones, each corresponding to a single free mode of vibration of the bar. Since the overtones are not in harmonic ratios with the fundamental, they may disrupt or substantially

alter the overall sensation of pitch. However by holding the bar at a nodal point all of the modes that do not have a node at that point are quickly damped, and the fundamental stands out more clearly.

### Appendix B: Estimation of the Q factor

The recorded impact sound must be inspected to find the peak corresponding to the first mode of vibration of the bar. The raw sound will most probably contain background noise. In order to obtain a simple waveform closer to the one for a damped harmonic oscillator it is useful to apply a narrow band-pass filter directly within Audacity through the built-in Filter-curve effect, which includes an intuitive interface to design the filter. We applied one-third octave band filter of order 3 that was enough to damp the residual signal from the first bending mode of vibration perpendicular to the direction of the strike.

Although internal damping is not due to viscous drag on a microscopic scale, the macroscopic effect results into an exponential decay in the oscillation amplitude, and therefore it can be modeled by adding an effective viscous term to the equation of motion for the free vibrations:

$$\frac{d^2x(t)}{dt^2} + 2\zeta\omega_0\frac{dx(t)}{dt} + \omega_0^2x(t) = 0, \quad (\text{B1})$$

with solution

$$x(t) = x_0 \sin(\omega t + \phi) \exp(-\zeta\omega_0 t), \quad (\text{B2})$$

where  $\omega_0$  is the undamped fundamental angular frequency,  $\zeta$  the damping ratio and  $\omega = \omega_0\sqrt{1 - \zeta^2}$ .

The damping ratio  $\zeta$  can be calculated analytically from the logarithmic decrement  $\delta$  of the signal

$$\delta = \frac{1}{n} \log \left( \frac{x_0}{x_n} \right), \quad (\text{B3})$$

where  $x_0$  and  $x_n$  are the amplitudes of the signal at a reference time and after  $n$  full periods of oscillation respectively. If the signal amplitude is represented in a dB scale, as it is often customary,  $\delta$  can be obtained from a simple linear fit of the envelope

$$\delta = \frac{0.1151}{n} (A_0 - A_n), \quad (\text{B4})$$

where  $A_i = 20 \log_{10}(x_i)$  are the signal amplitudes in dB. Then

$$\zeta = \frac{\delta}{\sqrt{4\pi^2 + \delta^2}} \approx \frac{\delta}{2\pi}. \quad (\text{B5})$$

Finally, damping is often quantified as the  $Q$  factor, which is simply

$$Q = \frac{1}{2\zeta} \approx \frac{\pi}{\delta}. \quad (\text{B6})$$

### Appendix C: Supporting information

1. Audio file *S1-Drop-sounds.mp4*. Sounds produced by dropping on the floor NiTiCu bars in their austenite and martensite phases.
2. Audio file *S2-Temperature-sounds.mp4*. Sounds of Iron and NiTiCu bars when temperature is lowered between 50 and 30 °C.

### Appendix D: Author Declarations

The authors have no conflicts to disclose.

---

\* carloandrea.rozzi@nano.cnr.it

<sup>1</sup> R. V. Solé, *Phase transitions* (Princeton University Press, 2011).

<sup>2</sup> J. P. Sethna, *Entropy, order parameters, and complexity* (Oxford University Press, 2004).

<sup>3</sup> J. F. Annett, *Superconductivity, Superfluids and Condensates* (Oxford University Press, 2006).

<sup>4</sup> A. Lisotti, V. D. Renzi, C. A. Rozzi, E. Villa, F. Albertini, and G. Goldoni, *Physics Education* **48**, 298 (2013), URL <https://dx.doi.org/10.1088/0031-9120/48/3/298>.

<sup>5</sup> Several solid-to-solid transition also occurs in water, but only at extreme conditions which are typically realized in some astronomical objects.

<sup>6</sup> K. Otsuka and X. Ren, *Progress in Materials Science* **50**, 511 (2005), ISSN 0079-6425, URL <http://www.sciencedirect.com/science/article/pii/S0079642504000647>.

<sup>7</sup> Christian, J. W., Olson, G. B., and Cohen, M., *J. Phys. IV France* **05**, C8 (1995), URL <https://doi.org/10.1051/jp4:1995801>.

<sup>8</sup> Clapp, P. C., *J. Phys. IV France* **05**, C8 (1995), URL <https://doi.org/10.1051/jp4:1995802>.

- <sup>9</sup> *Shape memory effect at nanolab.unimore.it*, accessed 2023-09-14, URL <https://www.youtube.com/watch?v=9DH-VOILyWE>.
- <sup>10</sup> J. Qi and L. Buechley, in *Proceedings of the SIGCHI Conference on Human Factors in Computing Systems* (Association for Computing Machinery, New York, NY, USA, 2012), CHI '12, p. 749–752, ISBN 9781450310154, URL <https://doi.org/10.1145/2207676.2207783>.
- <sup>11</sup> D. Amariei, D. Frunzaverde, I. Vela, and G. R. Gillich, *Procedia - Social and Behavioral Sciences* **2**, 5104 (2010), ISSN 1877-0428, innovation and Creativity in Education, URL <https://www.sciencedirect.com/science/article/pii/S1877042810008694>.
- <sup>12</sup> G. Song and R. Bannerot, in *2007 Annual Conference & Exposition* (ASEE Conferences, Honolulu, Hawaii, 2007), URL <https://peer.asee.org/development-of-an-interactive-shape-memory-alloy-demonstration-for-smart-materials-curriculum>.
- <sup>13</sup> F. Cichocki, P. Krulevitch, and L. Olson, *Flexible cannula comprising a nitinol strip jacketed by a flexible tube for medical applications* (2009), EP Patent App. EP20,080,253,500, URL <https://encrypted.google.com/patents/EP2055333A1?cl=un>.
- <sup>14</sup> R. Banks, *Single wire nitinol engine* (1984), US Patent 4,450,686, URL <http://www.google.com/patents/US4450686>.
- <sup>15</sup> G. Julien, *Nitinol impact absorbers* (2003), US Patent 6,530,564, URL <http://www.google.com/patents/US6530564>.
- <sup>16</sup> T. Schneider, *Polymer composite structure reinforced with shape memory alloy and method of manufacturing same* (2006), US Patent 6,989,197, URL <http://www.google.com/patents/US6989197>.
- <sup>17</sup> C. Fang and M. C. Yam, *Frontiers in Built Environment* **8** (2023), ISSN 2297-3362, URL <https://www.frontiersin.org/articles/10.3389/fbuil.2022.953273>.
- <sup>18</sup> W. J. Buehler and F. E. Wang, *Ocean Engineering* **1**, 105 (1968), ISSN 0029-8018, URL <https://www.sciencedirect.com/science/article/pii/002980186890019X>.
- <sup>19</sup> This fact was promptly noticed since early experiments by Buehler and Wiley<sup>43</sup>, who made good use of their ears as an aid to characterize the samples and to complement their measurements. Curiously, they have classified the sounds they perceived using vivid, yet fuzzy categories like “dull”, “slight ring”, “clear ring”, “sharp high frequency ring” and “transition”, but the analysis of such sounds was not deepened further.



- <sup>20</sup> K. R. C. Gisser, M. J. Geselbracht, A. Cappellari, L. Hunsberger, A. B. Ellis, J. Perepezko, and G. C. Lisensky, *Journal of Chemical Education* **71**, 334 (1994), URL <http://dx.doi.org/10.1021/ed071p334>.
- <sup>21</sup> D. J. Campbell, J. P. Peterson, and T. J. Fitzjarrald, *Journal of Chemical Education* **91**, 1684 (2014), ISSN 0021-9584, URL <https://doi.org/10.1021/ed500070j>.
- <sup>22</sup> F. C. Nix and D. MacNair, *Phys. Rev.* **60**, 597 (1941), URL <https://link.aps.org/doi/10.1103/PhysRev.60.597>.
- <sup>23</sup> H. M. Ledbetter and R. P. Reed, *Journal of Physical and Chemical Reference Data* **2**, 531 (1973), ISSN 0047-2689, [https://pubs.aip.org/aip/jpr/article-pdf/2/3/531/19257316/531\\_1\\_online.pdf](https://pubs.aip.org/aip/jpr/article-pdf/2/3/531/19257316/531_1_online.pdf), URL <https://doi.org/10.1063/1.3253127>.
- <sup>24</sup> Though in phase transitions we are used to associate the low-temperature phase with the more symmetric structure, this is not necessarily always the case. In fact, in our system, the high-temperature B2 phase has a formation enthalpy which is about 0.034 eV/atom larger than the low-temperature B19' phase (see Ref. 28), being therefore stabilized by entropy at sufficiently high-temperature.
- <sup>25</sup> L. C. Chang and T. A. Read, *Transactions of the American Institute of Mining Metallurgical and Petroleum Engineers* **189**, 47 (1951).
- <sup>26</sup> D. E. Hodgson and R. J. Biermann, *ASM Handbook: Nonferrous Alloys and Special-Purpose Materials* (ASM International, 1990), vol. 2, p. 2524, ISBN 978-0-87170-378-1, URL <https://dl.asminternational.org/handbooks/edited-volume/14/chapter-abstract/188049/Shape-Memory-Alloys>.
- <sup>27</sup> W. J. Buehler, J. V. Gilfrich, and R. C. Wiley, *Journal of Applied Physics* **34**, 1475 (1963), URL <http://dx.doi.org/10.1063/1.1729603>.
- <sup>28</sup> W. S. Ko, B. Grabowski, and J. Neugebauer, *Phys. Rev. B - Condens. Matter Mater. Phys.* **92**, 1 (2015), ISSN 1550235X, URL <https://journals.aps.org/prb/abstract/10.1103/PhysRevB.92.134107>.
- <sup>29</sup> K. Otsuka and C. M. Wayman, eds., *Shape memory materials* (Cambridge University Press, 1999), ISBN 9780521663847, URL <http://www.cambridge.org/it/academic/subjects/engineering/materials-science/shape-memory-materials#gVjol5kZADu6G7fF.97>.
- <sup>30</sup> in *Phase Transformations*, edited by S. Banerjee and P. Mukhopadhyay (Pergamon, 2007), vol. 12 of *Pergamon Materials Series*, pp. 257–376, URL <https://www.sciencedirect.com/>

science/article/pii/S1470180407800575.

- <sup>31</sup> *Audacity(R)*, accessed 2023-09-14, URL <http://audacity.sourceforge.net>.
- <sup>32</sup> For sake of comparison, the closest tone to  $A_5$  in western music would be 50 Hz lower ( $A_5^b$ ) or higher ( $A_5^\sharp$ ).
- <sup>33</sup> From the standard unit cell parameters in the tetragonal and monoclinic phases of NiTi reported in Otsuka and Ren<sup>6</sup> one obtains a theoretical density of 6.46 g/cm<sup>3</sup> for the austenite, and 6.17 g/cm<sup>3</sup> for the martensite. This would result in an effective thermal coefficient of the order of 10<sup>-5</sup> °C<sup>-1</sup>.
- <sup>34</sup> M.-X. Wagner and W. Windl, *Acta Materialia* **56**, 6232 (2008), ISSN 1359-6454, URL <https://www.sciencedirect.com/science/article/pii/S1359645408006083>.
- <sup>35</sup> F. Mazzolai, A. Biscarini, R. Campanella, B. Coluzzi, G. Mazzolai, A. Rotini, and A. Tuissi, *Acta Materialia* **51**, 573 (2003), ISSN 1359-6454, URL <https://www.sciencedirect.com/science/article/pii/S1359645402004391>.
- <sup>36</sup> A. Rotini, A. Biscarini, R. Campanella, B. Coluzzi, G. Mazzolai, and F. Mazzolai, *Scripta Materialia* **44**, 719 (2001), ISSN 1359-6462, URL <https://www.sciencedirect.com/science/article/pii/S1359646200006722>.
- <sup>37</sup> Actually the martensite phase also has larger porosity than the austenite one, and in fact its surface appears rougher and less polished. However this has no noticeable effect for our sample sizes.
- <sup>38</sup> S. Saedi, E. Acar, H. Raji, S. E. Saghaian, and M. Mirsayar, *Journal of Alloys and Compounds* **956**, 170286 (2023), ISSN 0925-8388, URL <https://www.sciencedirect.com/science/article/pii/S092583882301589X>.
- <sup>39</sup> I. Yoshida, D. Monma, K. Iino, K. Otsuka, M. Asai, and H. Tsuzuki, *Journal of Alloys and Compounds* **355**, 79 (2003), ISSN 0925-8388, proceedings of the International Symposium on High Damping Materials, URL <https://www.sciencedirect.com/science/article/pii/S0925838803002809>.
- <sup>40</sup> J. V. Humbeeck and S. Kustov, *Smart Materials and Structures* **14**, S171 (2005), URL <https://dx.doi.org/10.1088/0964-1726/14/5/001>.
- <sup>41</sup> *Nanolab*, video description of the procedure (in Italian), Accessed 2023-09-14, URL <https://www.nanolab.unimore.it/laboratori/lab-nitinolo/transizioni-di-fase-2/transizioni-di-fase-1-resistivita-e-allungamento/>.

- <sup>42</sup> J. W. S. Lord Rayleigh, *The Theory of Sound* (MacMillan & co., 1877), reprint Dover Publications, New York, (1945).
- <sup>43</sup> W. J. Buehler and R. C. Wiley, Tech. Rep. AD0266607, U.S. Naval Ordnance Laboratory, White Oak MD (1961), URL <https://apps.dtic.mil/sti/citations/tr/AD0266607>.

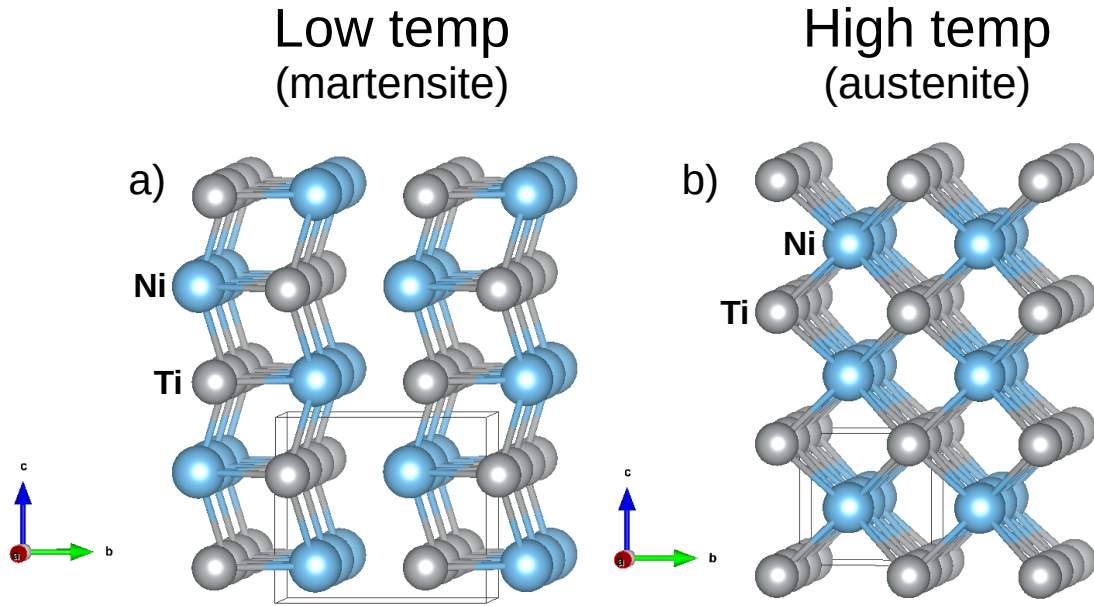


FIG. 1. Lattice geometry of a) twinned martensite (B19' phase, monoclinic crystal lattice, space group 11) and b) austenite (B2 phase, cubic lattice, space group 221). Ni and Ti atoms are indicated in light blue and gray respectively. The arrows indicate the  $b$  and  $c$  crystallographic axes, while the  $a$  axis is pointing out of the page plane. The unit cells are delimited by the thin lines, and, for clarity of representation, the pictures show supercells including  $3 \times 2 \times 3$  unit cells each. The sticks are added to highlight the stacked patterns. They do not indicate chemical bonds.

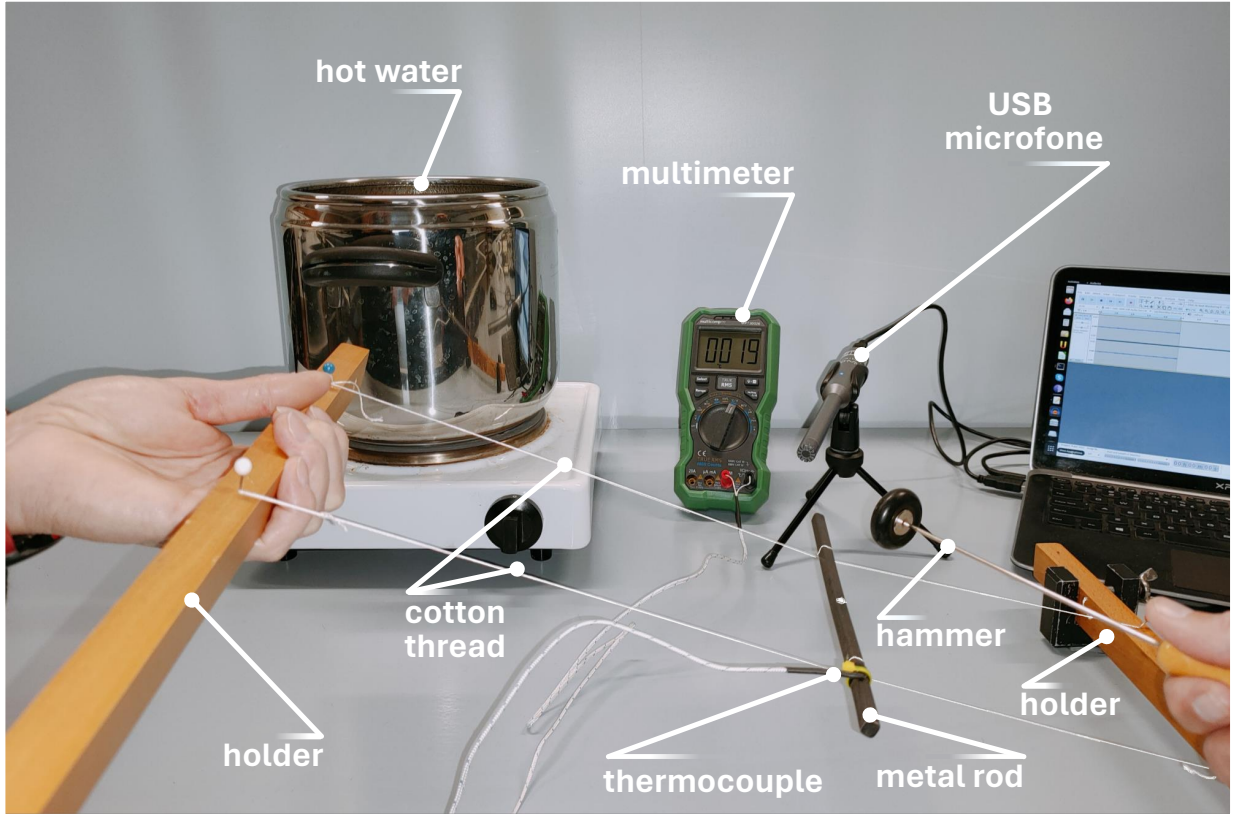


FIG. 2. Photo of the experimental setup and procedure. The bar (either the Nitinol or the Fe bar) is tied to two rigid holders with cotton threads passing at the nodal planes. A thermocouple is fixed to the bar and the temperature is read by a multimeter. Using the holders, the bar is first moved into a hot water bowl, maintained at fixed temperature, to thermalize. Then, the bar is quickly extracted from water and held suspended with the holders. As the bar gradually cools, the operator may repeatedly take note of (or read aloud for recording) the temperature from the multimeter and gently hit the bar with a rubber hammer. The sound trace is recorded through a microphone connected to a computer to be analyzed.

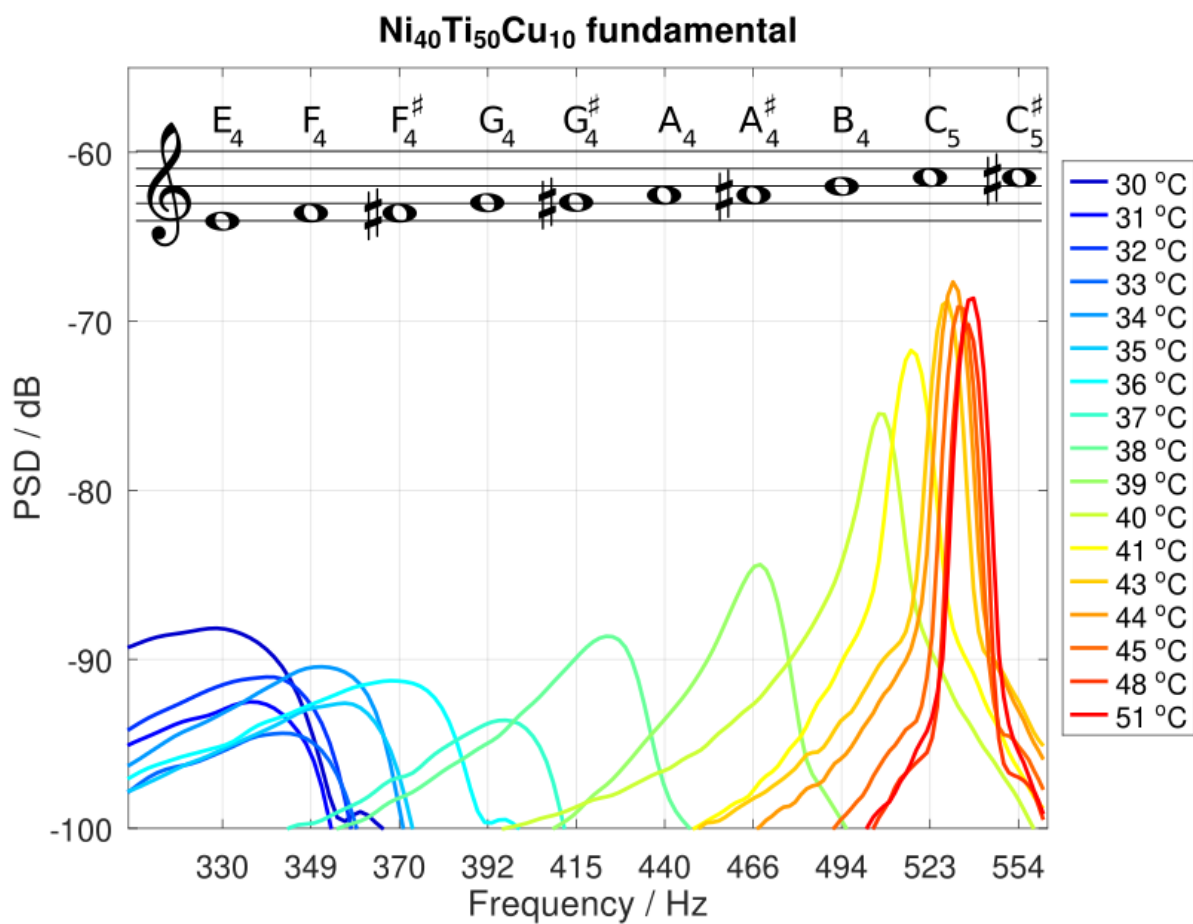


FIG. 3. Power spectral densities (PSD) of the fundamental modes of the NiTiCu bar at measured temperatures. At the top we report the musical notation of the notes at the frequencies denoted by the vertical grid lines.

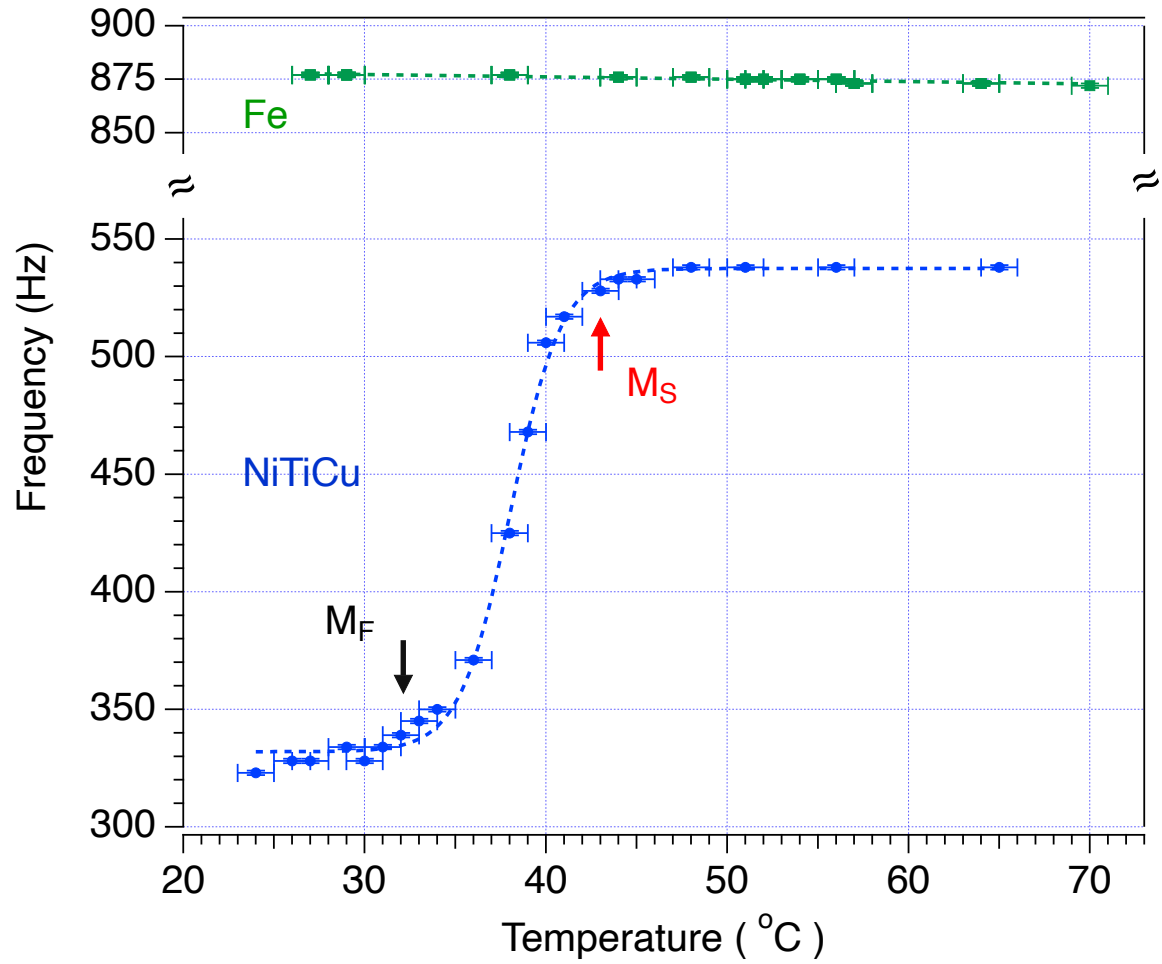


FIG. 4. Measured temperature dependence of the frequency of the fundamental mode of vibration of Iron (top) and Nitinol (bottom) rods upon cooling. The arrows mark the estimated Martensite start ( $M_S$ ) and end ( $M_F$ ) temperatures at 43 and 32 °C respectively. The superimposed dashed lines are guides for the eye.

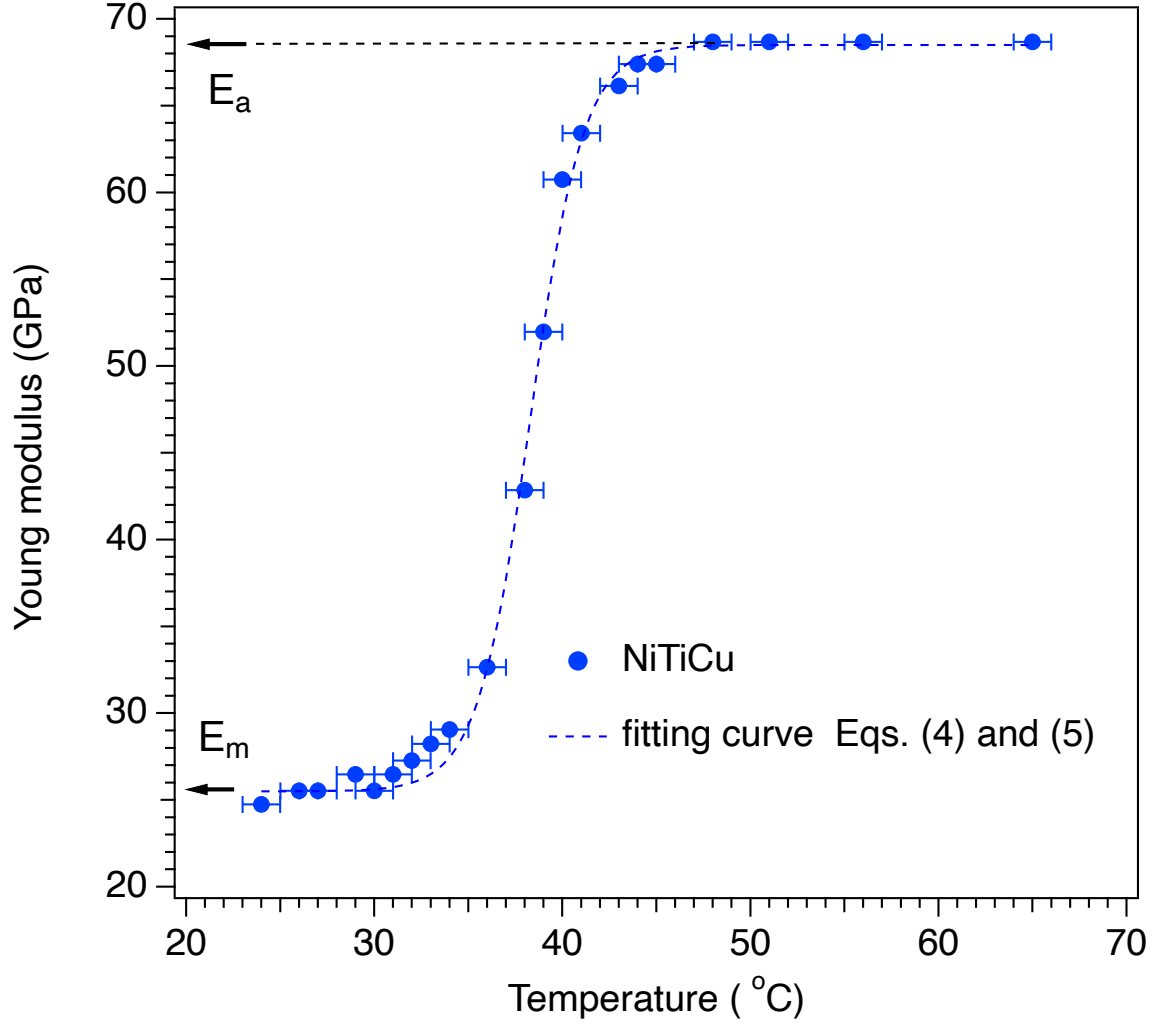


FIG. 5. Variation of the Young's modulus, as evaluated from our experiments, as a function of temperature. The fitting curve (dashed line) is the logistic function, as indicated in eqs. 4 and 5 with parameters  $T_m = 38.3$  °C and  $k = -1.4$  (°C) $^{-1}$ . The values of  $E_a = (69 \pm 1)$  GPa and  $E_m = (26 \pm 1)$  GPa, as obtain by the fitting procedure, are also indicated by horizontal arrows.



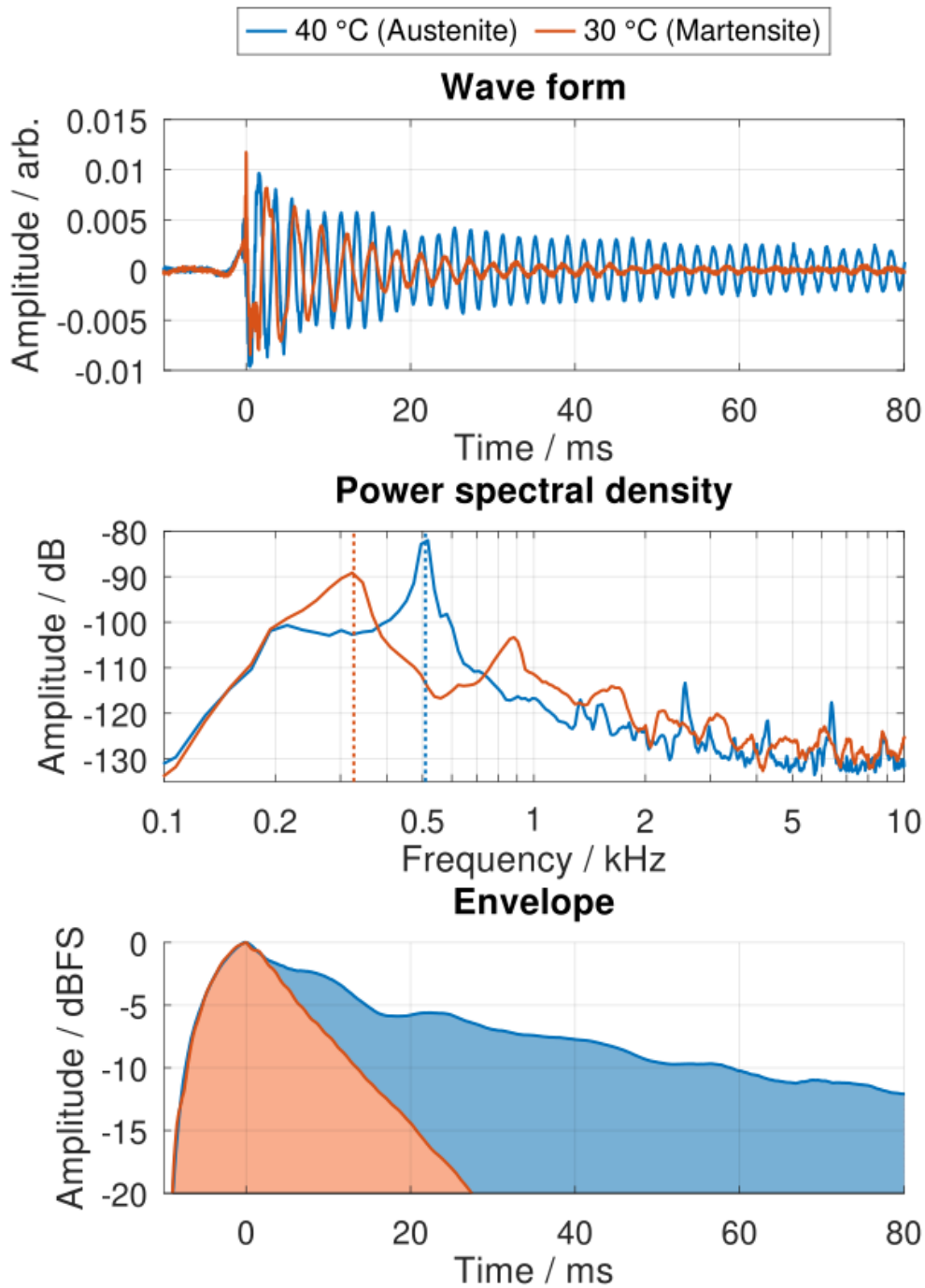


FIG. 6. Two selected sounds of the NiTiCu bar at 40 °C (austenite) and 30 °C (martensite), i.e. close to the beginning and end of the martensitic PT. Top: time-domain waveforms. Middle: Power spectral densities highlighting the presence of a fundamental peak (marked with broken lines) and a few overtones. Bottom: waveform envelopes highlighting the different decay times.

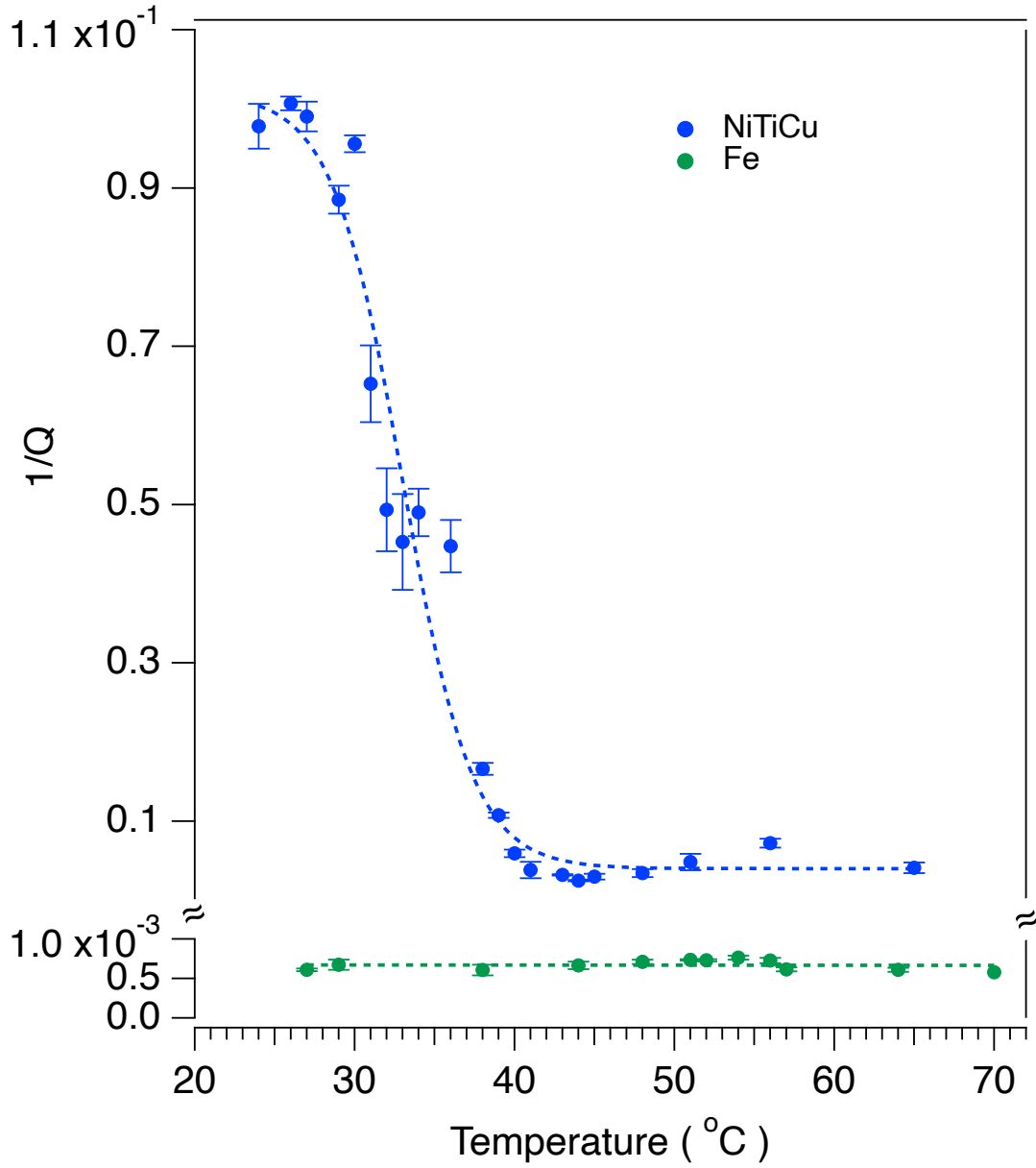


FIG. 7. Temperature dependence of the inverse Q factor as evaluated from the measured sound spectra of the fundamental for Nitinol (blue) and Iron (green) rods. The corresponding dashed lines are guides for the eyes.